NeuroImage: Clinical 36 (2022) 103173

Contents lists available at ScienceDirect

NeuroImage: Clinical

journal homepage: www.elsevier.com/locate/ynicl

Use of magnetic resonance elastography to gauge meningioma intratumoral consistency and histotype

Yu Shi [a,1], Yunlong Huo [b,1], Chen Pan [a,1], Yafei Qi [b], Ziying Yin [c], Richard L. Ehman [c], Zhenyu Li [a], Xiaoli Yin [a], Bai Du [a], Ziyang Qi [a], Yang Hong [d,*]

[a] Department of Radiology, Shengjing Hospital of China Medical University, Shenyang, Liaoning Province, PR China
[b] Department of Pathology, Shengjing Hospital of China Medical University, Shenyang, Liaoning Province, PR China
[c] Department of Radiology, Mayo Clinic College of Medicine, Rochester, MN, United States
[d] Department of Neurosurgery, Shengjing Hospital, China Medical University, Shenyang, PR China

ARTICLE INFO

Keywords:
Meningiomas
Magnetic resonance imaging
Elastography
Mechanical properties
Stiffness

ABSTRACT

Objective: To determine whether tumor shear stiffness, as measured by magnetic resonance elastography, corresponds with intratumoral consistency and histotype.

Materials and methods: A total of 88 patients with 89 meningiomas (grade 1, 74 typical [13 fibroblastic, 61 non-fibroblastic]; grade 2, 12 atypical; grade 3, 3 anaplastic) were prospectively studied, each undergoing preoperative MRE in conjunction with T1-, T2- and diffusion-weighted imaging. Contrast-enhanced T1-weighted sequences were also obtained. Tumor consistency was evaluated as heterogeneous or homogenous, and graded on a 5-point scale intraoperatively. MRE-determined shear stiffness was associated with tumor consistency by surgeon's evaluation and whole-slide histologic analyses.

Results: Mean tumor stiffness overall was 3.81+/-1.74 kPa (range, 1.57–12.60 kPa), correlating well with intraoperative scoring ($r = 0.748$; $p = 0.001$). MRE performed well as a gauge of tumor consistency (AUC = 0.879, 95 % CI: 0.792–0.938) and heterogeneity (AUC = 0.773, 95 % CI: 0.618–0.813), significantly surpassing conventional MR techniques (DeLong test, all $p < 0.001$ after Bonferroni adjustment). Shear stiffness was independently correlated with both fibrous content (partial correlation coefficient = 0.752; $p < 0.001$) and tumor cellularity (partial correlation coefficient = 0.547; $p < 0.001$). MRE outperformed other imaging techniques in distinguishing fibroblastic meningiomas from other histotypes (AUC = 0.835 vs 0.513 ~ 0.634; all $p < 0.05$), but showed limited ability to differentiate atypical or anaplastic meningiomas from typical meningiomas (AUC = 0.723 vs 0.616 ~ 0.775; all $p > 0.05$). Small (<2.5 cm, n = 6) and intraventricular (n = 2) tumors displayed inconsistencies between MRE and surgeon's evaluation.

Conclusions: The results of this prospective study provide substantial evidence that preoperative evaluation of meningiomas with MRE can reliably characterize tumor stiffness and spatial heterogeneity to aid neurosurgical planning.

1. Introduction

Meningiomas are the most common extra-axial brain neoplasms, accounting for approximately 30 % of all primary intracranial tumors (Riemenschneider et al., 2006). Tumor consistency is an important factor in determining their surgical outcomes. Firmer tumors ostensibly should be more amenable to conventional open approaches, whereas minimally invasive procedures would be favored for softer tumors. A

Abbreviations: MRE, magnetic resonance elastography; ROC, receiver operating characteristic; AUC, areas under curves; kPa, kilopascals; DWI, diffusion-weighted imaging; TR, repetition time; TE, echo time; Gd-DTPA, gadolinium diethylenetriaminepentaacetic acid; FLAIR, fluid-attenuated inversion recovery; ROIs, regions of interest; HE, hematoxylin eosin; IHC, Immunohistochemistry; EMA, epithelial membrane antigen; PR, progesterone receptor; MVD, microvascular density; SD, standard deviation; IQR, interquartile range; ICC, intraclass correlation coefficient.

* Corresponding author at: Department of Neurosurgery, Shengjing Hospital, China Medical University, No. 36, Sanhao Street, Heping District, Shenyang 110004, PR China.
E-mail address: hongyangcmu@hotmail.com (Y. Hong).

[1] Yu Shi, Yunlong Huo and Chen Pan contribute equally to this work.

https://doi.org/10.1016/j.nicl.2022.103173
Received 3 May 2022; Received in revised form 24 August 2022; Accepted 25 August 2022
Available online 29 August 2022

firm consistency, regularly encountered in meningiomas with more fibrous content (eg, fibroblastic histotypes) makes tumor removal difficult, especially skull base meningiomas or intraventricular meningiomas (Alyamany et al., 2018; Cepeda et al., 2021; Hoover et al., 2011; Itamura et al., 2018; Kashimura et al., 2007; Phuttharak et al., 2018; Shiroishi et al., 2016; Sitthinamsuwan et al., 2012; Smith et al., 2015; Smith et al., 2017; Yamada et al., 2021; Yao et al., 2018). Preoperative knowledge of tumor consistency may ultimately help guide operative decisions to conduct planned staged resections, anticipate subtotal resections, or consider minimally invasive procedures (ie, endoscopic aspiration and suction) (Zada et al., 2013). For those meningiomas of variable compositions, a means of determining spatial intratumoral inconsistencies would be an ideal surgical planning asset.

Meningiomas of all grades do share some basic imaging features, namely their well-circumscribed/solid configurations, dural-based growth, and affinity for enhancement. Nonetheless, it is still unclear whether differing grades or subtypes of meningiomas may be accurately diagnosed using conventional magnetic resonance (MR) imaging (Chen et al., 1992) (Hsu et al., 2010). Imaging-based elastography, whether by ultrasound or by MR elastography (MRE), is already a proven tool for direct quantification of intratumoral stiffness (Chakraborty et al., 2012). However, ultrasound technology may only be used once the skull is opened at surgery, whereas MRE is uniquely capable of preoperatively determining intratumoral consistency. MRE is a MR-based technique that measures propagation of vibration-induced displacement and viscoelastic mechanical properties in tissues of interest. It has served successfully in assessing liver fibrosis, and several earlier studies have pioneered its use in preoperative appraisals of meningiomas, correlating results with intraoperative observations (Hughes et al., 2015; Murphy et al., 2013a; Takamura et al., 2021; Xu et al., 2007). Unfortunately, there were too few available cases (12–18 only), and the histological factors determining shear stiffness have not yet been reported.

The goals of this prospective study were as follows: (1) determine whether MRE helps determine intratumoral firmness and spatial heterogeneity preoperatively; (2) assess whole-slide histologic features in relation to MRE-based shear stiffness; and (3) explore MRE as a preoperative gauge of meningioma grade and histotype in a cohort of 88 patients.

2. Material and methods

2.1. Patient characteristics

This prospective single-center study received institutional review board approval and complied with the Health Insurance Portability and Accountability Act (HIPPA). Once authorized, we enrolled inpatients between October 2017 and November 2021 for preoperative MRE studies of presumptive meningiomas. Each subject was scheduled for surgical planning in the Department of Neuroradiology at a local institution, recruited by the operating surgeons. MRE imaging proceeded after obtaining written informed consent. Grounds for exclusion were the following: (1) failure to operate after MRE study (eg, small tumors not requiring removal); (2) preoperative endovascular embolization in advance of MRE; (3) clinically confirmed local meningioma recurrence; (4) small tumors still requiring surgery but insufficient for MRE analysis (<1.5 cm); (5) suboptimal wave image quality (including motion artifacts or low illumination of wave images); and (6) unavailability of histologic evaluation.

Ultimately, 88 patients with 89 meningiomas proved acceptable for study. Diagnosis of meningioma was confirmed in each instance by histologic examination of surgically resected tissue samples.

2.2. MR image acquisition

All MRE studies involved modified single-shot spin-echo echo-planar imaging pulse sequences generated via 3 T MRI system (Signa Excite; GE Healthcare, Chicago, IL, USA). Shear waves were introduced intracranially, using a soft, pillow-like pneumatic driver placed beneath each subject's head (Hughes et al., 2015; Murphy et al., 2013a). This tailored head driver was provided by Mayo Clinic through a mutual service agreement. Both axial and sagittal MRE images were acquired for 3D mapping of tumor consistencies. The power amplitude of mechanical waves was 25 %, adjusted from 20 to 30 %. Imaging parameters were as follows: vibration frequency, 60 Hz; repetition time (TR)/echo time (TE), 3600/62 ms; field of view, 24 cm; acquisition matrix, 72 × 72; slice thickness, 3 mm; contiguous axial slices, 48; motion-encoding gradient, 18.2 ms (each side of refocusing RF pulse); 6 motion encoding directions: ±x, ±y, ±z; and phase offsets, 8 (evenly spaced over one period of 60-Hz motion). Approximately 20 min of imaging time was needed for MRE portions of exams.

Routine MR pulse sequences included pre-contrast axial T1- (T1W), T2- (T2W), and diffusion-weighted (DWI) imaging (b value, 1000 *sec/mm*^{2}), as well as fluid-attenuated inversion recovery (FLAIR) imaging. Contrast-enhanced T1W sequences were obtained after administering gadolinium diethylenetriaminepentaacetic acid (Gd-DTPA) contrast (Magnevist, 0.1 mmol/kg; Bayer HealthCare, Leverkusen, Germany), as detailed in Appendices.

2.3. Surgical procedures and intraoperative tumor consistency assessments

Two surgeon specialists in brain surgery (25 and 38 years, respectively) primarily conducted all surgical resections, their intraoperative impressions of tumor consistency serving as reference standards. During these evaluations, another similarly experienced neurosurgeon (18 years) recorded detailed notes. All the above were quite familiar with the scope of meningioma presentations. While blinded to MRE results, the principals were tasked with intraoperative gauging of tumor consistency and heterogeneity. If deemed consistent, and the same surgical instrument worked well throughout, a tumor was considered homogenous. Heterogenous tumors showed tissue inconsistencies, requiring different instruments for complete removal. Their approximate anatomic locations were noted for later correlation with MRE.

Using a 5-point scale described by Zada et al (Zada et al., 2013), grading of tumor consistency during resection was as follows: grade 1, very soft (softest consistency subset, amenable to internal debulking by suction alone); grade 2, relatively soft, (partial debulking achievable by suction, with added resection of retained interspersed fibrous stroma); grade 3, intermediate (tumors not freely relenting to suction, necessitating some degree of mechanical debulking); grade 4, firm (posing a surgical challenge, despite internal debulking; or grade 5, very firm (approaching consistency of bone, so the process of internal debulking and capsular folding generally fails).

2.4. Image and data processing

Quantified tissue viscoelastic shear properties were based on measured displacement fields (Muthupillai et al., 1995; Papazoglou et al., 2008; Sinkus et al., 2005). Assuming the tissue to be linear, isotropic, locally homogeneous, and viscoelastic, we calculated the complex shear modulus using previously described direct inversion methods (Clayton et al., 2012; Manduca et al., 2001; Murphy et al., 2013b). Several preprocessing steps were taken before direct inversion, as detailed in Appendices (Hughes et al., 2015; Murphy et al., 2013a). Shear stiffness was to describe the magnitude (absolute value) of the complex shear modulus.

Tumor consistency evaluations included intratumoral tumor heterogeneity assessments and shear stiffness determinations in kilopascals (kPa). According to Hughes et al, any tumor with 20 % regions of interest (ROIs) showing distinctly different stiffness values qualified as heterogeneous. MRE measures shear stiffness by calculating median stiffness in each ROI. Thus, heterogenous tumors must demonstrate at

least 2 ROIs. Tumor ROIs were drawn on every section of the magnitude image registered to the MR elastogram by two radiologists (both > 10 years of experience in neuroradiology), working independently and blinded to clinical information. Any resultant discrepancies were resolved through discussion, reaching a consensus. Tumor stiffness was calculated as the median shear stiffness of voxels contained in each ROI and averaged across all ROIs.

2.5. Pathologic assessments

Once surgical specimens were processed, tissue samples were sectioned at 5 μm, deparaffinized, and rehydrated for routine hematoxylin-eosin (HE) staining. Immunohistochemical (IHC) markers were also analyzed, specifically epithelial membrane antigen (EMA), progesterone receptor (PR), and Ki-67 protein (MIB-1 monoclonal antibody; ZSGB-Bio, Beijing, China) and CD31 for Microvascular density (MVD). Most meningiomas are diffusely positive for EMA, attesting to the dual mesenchymal/epithelial nature of meningothelial cellular constituents. An elevated proliferation index (by Ki-67 immunostain) and loss of PR expression at high (200x) magnification are features of higher grade tumors. All slide preparations were manually examined by two experienced pathologists (over 13 years and 18 years, respectively), assigning World Health Organization (WHO) grades and histotypes by light microscopy (BX53; Olympus, Tokyo, Japan). Both experts were blinded to clinical and MR imaging data.

2.6. Digital imaging analysis

HE-stained tissue slides from various tumor areas were scanned digitally using a NanoZoomer 2.0-RS whole-slide image scanner (Hamamatsu Photonics, Hamamatsu City, Shizuoka, Japan), Zeiss Zen 3.0 (blue edition; Carl Zeiss AG, Oberkochen, Germany) software, and a HV viewer with a pixel-level (0.19 μm × 0.19 μm) specimen resolution at 40x magnification. ROIs of tumors with differing stiffness values corresponded with differing areas on digital histologic images by observing the images at 1x, 5x and 10x magnification. Digital images of 2270 × 1249 pixels (exported at 40x magnification) were obtained for each ROI for quantitative analysis. At least three photos were taken of each ROI, recording the mean. Quantitative histologic parameters included tumor cellularity (expressed as mean cell count), fibrous content (ie, collagen proportionate area [CPA], expressed as percentage), vascular density and Ki-67. Mean cell count and tumor CPA, vascular density and Ki-67 at 40x were obtained by computer-assisted analysis using Image-Pro Plus (v6.0.0.260; Media Cybernetics Inc, Rockville, MD, USA).

2.7. Statistical analysis

Categorical data were expressed as counts or percentages, reporting continuous data as mean ± standard deviation (SD) for normal distributions or as median (the 1st and 3rd interquartile range [IQR]) values for non-normal distributions (Shapiro-Wilk test). Chi-squared test was applied to test differences in proportions. We assessed differences in atypical, typical, fibroblastic, and other meningioma histotypes (based on MR imaging parameters) using nonparametric Mann-Whitney *U* test. Bonferroni correction was invoked to adjust *p*-values in multiple comparisons. Demographic data and specific tumor locations were subject to descriptive analysis. The relation between measured shear stiffness and tumor cellularity or fibrous content was examined via Spearman's rank correlation coefficient test (*r*), a range of 0.5–1.0 denoting significance for both. To evaluate interrater agreement, intraclass correlation coefficient (ICC) served for numerical data and Cohen's kappa for nominal and ordinal data, interpreting kappa values (ie, level of agreement) as follows: 0–0.2, slight; 0.2–0.4, fair; 0.4–0.6, moderate; 0.6–0.8, substantial; 0.8–1.0, near perfect.

Receiver operating characteristic (ROC) curve analyses were conducted to compare levels of diagnostic performance by MR parameters in detecting tumor firmness and heterogeneity and in differentiating meningioma subsets (grade 2–3 vs grade 1 and fibroblastic vs other typical meningiomas). Areas under ROC curves (AUCs) were compared using DeLong test. All statistical analyses were driven by standard software, including SPSS v25.0 (IBM Corp, Armonk, NY, USA), Prism 7.0 (GraphPad Software Inc, San Diego, CA, USA), and MedCalc (MedCalc Software ltd, Ostend, Belgium), setting significance at $p < 0.05$.

3. Results

3.1. Demographics

Table 1 shows demographic, presentational, and tumor characteristic distributions within the study population. Meningioma was confirmed in each patient through histologic examination of surgically resected tissue samples. The pathologic diagnoses rendered included 74

Table 1
Patient demographics, presenting symptoms, and tumor characteristics.

Parameter	Mean or Number
Age, yrs	
Mean (range)	61.6 (21–77)
Sex	
Male	35 (39.8)
Female	53 (60.2)
Symptoms	
Headache and dizziness	36 (40.9)
Epilepsy	6 (6.8)
Speech disorder	6 (6.8)
Visual disorder	10 (11.4)
Hearing disorder and tinnitus	5 (5.7)
Limb weakness	8 (9.1)
Gait disturbance	6 (6.8)
Others	11 (12.5)
Tumor size, cm	
Mean (range)	4.04 (1.7–8.8)
Tumor location	
Convexity	43 (48.3)
Parafalcine	8 (9.0)
Tentorial	4 (4.5)
Anterior fossa	6 (6.7)
Posterior fossa	8 (9.0)
Cerebellopontine angle	5 (5.6)
Sellar region	7 (7.9)
Intraventricular	2 (2.2)
Others	6 (6.7)
WHO tumor grade	
Grade 1	74 (83.1)
Fibroblastic	13 (18.9)
Transitional	29 (37.8)
Meningothelial	29 (39.2)
Angiomatous	2 (2.7)
Microcystic	1 (1.4)
Grade 2	12 (13.5)
Grade 3	3 (3.4)
Surgeon's evaluation	
Tissue composition	
Homogeneous	57 (64)
Heterogeneous	32 (36)
Consistency score*	
1: Extremely soft	7 (7.9)
2: Soft	21 (23.6)
3: Intermediate	24 (27.0)
4: Firm	27 (30.3)
5: Extremely Firm	10 (11.2)
Operation	
Complete resection	26 (29.2)
Partial resection	15 (16.9)
Piecemeal resection	48 (53.9)

Data expressed as n (%) unless otherwise specified.
*Grading scale based on system of Zada et al for standardizing tumor consistency.

typical (grade 1) meningiomas (men, 26; women, 48; mean age, 62.6 ± 11.5 years; age range, 21–73 years), 12 atypical (grade 2) meningiomas (men, 8; women, 4; mean age, 64.3 ± 5.5 years; age range, 48–77 years) and 3 anaplastic (grade 3) meningiomas (men, 1; women, 2; mean age, 58.3 ± 5.5 years; age range, 52–62 years). Typical meningiomas encompassed fibroblastic (n = 13), transitional (n = 29), meningothelial (n = 29), angiomatous (n = 2), and microcystic (n = 1) histotypes.

Mean shear stiffness for meningiomas overall was 3.81 ± 1.74 kPa (range, 1.57–12.6 kPa) with inter-rater ICC of 0.91(95 %CI: 0.87 to 0.94). The stiffest tumor (12.6 kPa), situated at the left convexity, and the softest tumor (1.57 kPa), occupying the sellar area, are both depicted in Fig. A1. As reference values, the mean stiffness values of cerebrum and cerebellum were 2.63 ± 0.43 kPa and 2.17 ± 0.24 kPa, respectively.

3.2. MRE versus intraoperative findings

In the course of study, a significant correlation emerged between MRE-determined shear stiffness and intraoperative consistency scores (r = 0.748; $p < 0.001$) (A). Distributions of shear stiffness among tumor grades and histotypes are shown in Fig. 1B and 1C. Preoperative MRE studies characterized most tumors (65/89, 73 %) as homogeneous, rather than heterogenous (24/89, 27 %), as did surgical evaluations (homogeneous: 57/89, 64 %; heterogeneous: 32/89, 36 %; kappa = 0.738, 95 % CI: 0.590–0.886, $p < 0.001$). Fig. 2 demonstrates a transitional meningioma of heterogenous consistency, showing the corresponding signal intensity on routine MR images. MRE and surgical evaluations also revealed distinctly soft and hard portions within one tumor. MRE-derived shear stiffness achieved an AUC value of 0.773 (95 % CI: 0.672–0.855; $p < 0.001$) in identifying heterogenous and homogenous meningiomas.

During surgical evaluations, 61 tumors (69 %) were designated firm or firm in part (averagely scored as 3–5 of tumor consistency), compared with 55 tumors (62 %) by MRE, indicating substantial agreement between surgical and MRE findings (kappa = 0.754, 95 % CI: 0.612–0.896; $p < 0.001$) (Figs. A2 and A3). There were 10 discordant assessments, including 8 false-negative tumors with firm areas. Six of these were small tumors (<2.5 cm) showing good wave illumination (Fig. A2), and 2 were intraventricular tumors, the wave illumination poor. The other 2 cases were false positives, erroneously shown to have firm areas (mean stiffness: 7.2 kPa and 6.1 kPa, respectively). MRE achieved an AUC of 0.879 (95 % CI: 0.792–0.938; $p < 0.001$) in detecting firm areas within tumors with a cutoff value of 5.1 kPa, surgical evaluation being the reference point. In both tasks, MRE outperformed all other conventional MR techniques (all $p < 0.001$ after Bonferroni adjustment, DeLong test) (Fig. 1D, Table 2).

3.3. MRE versus histologic findings

Mean tumor cellularity was 1668 ± 873 (range: 706–6450) at 40x magnification, showing moderate positive correlation with shear stiffness in meningiomas ($r = 0.618$; $p < 0.001$). Mean CPA was 25.8 ± 19.6 % (range: 0–87 %), again correlating significantly with shear stiffness in this context ($r = 0.768$; $p < 0.001$). Both mean Ki-67 (7.9 ± 14.6 %, range: 0.5 %~80 %) and MVD (3.1 ± 2.2 %) showed no significant correlation with shear stiffness in meningiomas (both $p > 0.05$). By linear regression analysis, both tumor cellularity ($r_{partial} = 0.547$) and fibrous content ($r_{partial} = 0.752$) independently contributed to shear stiffness (adjusted $r^2 = 0.648$; $p < 0.001$).

Representative images of various WHO meningioma grades and histotypes are shown in Figs. 3-6. The median shear stiffness values (IQR) in typical, atypical, and anaplastic tumors were 3.32 (IQR: 2.58, 4.21) kPa, 4.24 (IQR: 3.70, 4.94) kPa, and 4.40 (IQR: 3.5, 5.03) kPa, respectively, indicating no significant differences among them (p = 0.064). Shear stiffness differed significantly ($p = 0.01$) in meningiomas of grades 1 and 2, but there was no significant difference between grades 1 and 3 ($p = 0.15$) or between grades 2 and 3 ($p = 0.89$) (Fig. 1B). Among

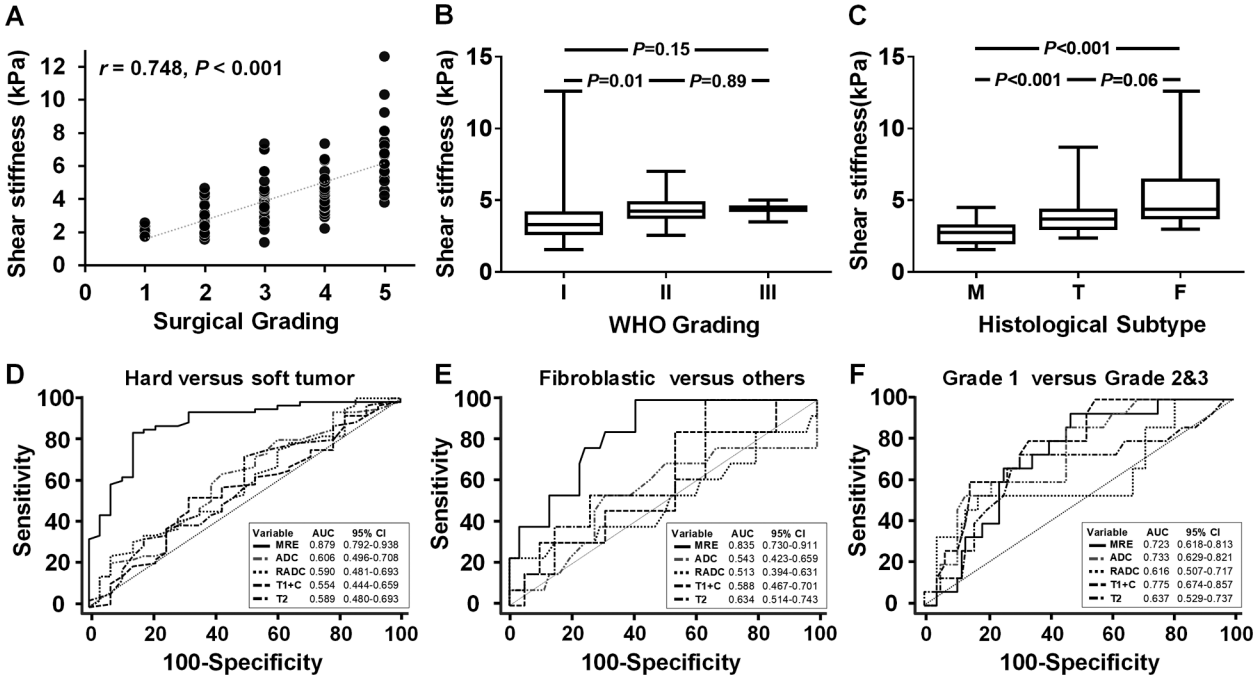

Fig. 1. **(A)** Spearman's correlation test, indicating strong correlation between shear stiffness level and grading by surgeon ($r = 0.748$; $p < 0.001$); **(B)** Shear stiffness of meningiomas stratified by World Health Organization (WHO) grade, pairwise comparisons (Mann-Whitney U test) showing significant difference between grades 1 and 2 ($p = 0.01$), but not between grades 1 and 3 ($p = 0.15$) or grades 2 and 3 ($p = 0.89$); **(C)** Shear stiffness of three main WHO grade 1 meningioma histotypes (T, transitional; M, meningothelial; F, fibroblastic), pairwise comparisons indicating significant difference in mean stiffness for T vs M ($p < 0.001$) and for M vs F ($p < 0.001$), but not for T vs F ($p = 0.06$); **(D-F)** Composite graph of receiver operating characteristic (ROC) curves comparing performance of shear stiffness with other conventional imaging techniques in identifying firm, fibroblastic, and grade 2–3 meningiomas, respectively. Traditional imaging measures included tumor apparent diffusion coefficient (ADC), relative ADC (mass ADC/brain ADC), signal intensity on T2-weighted imaging and contrast-enhanced T1-weighted imaging.

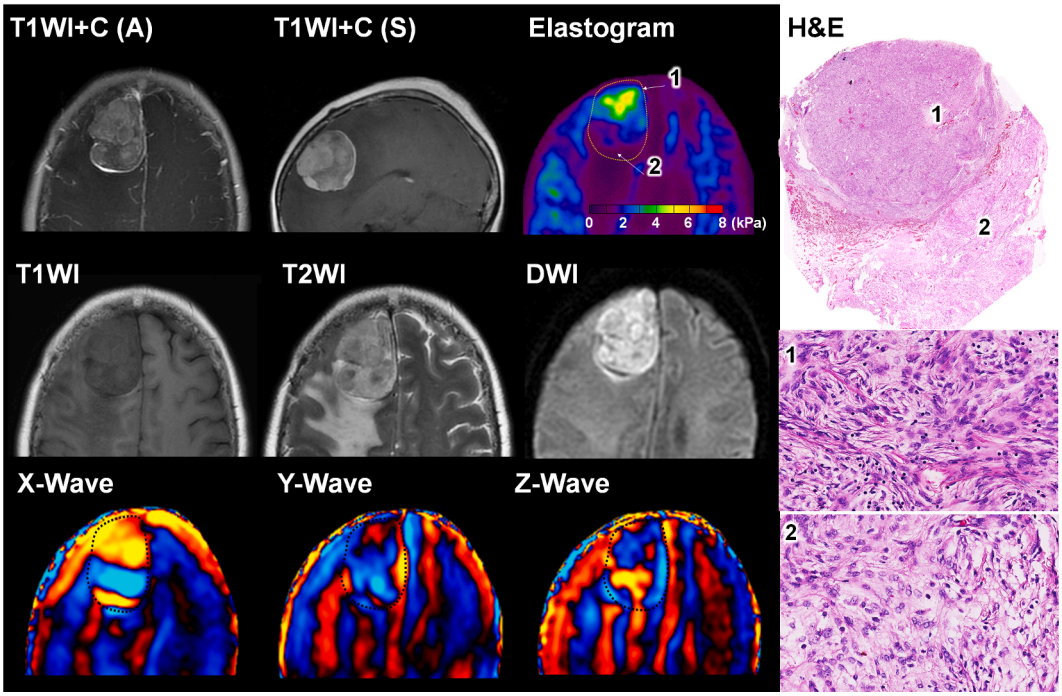

Fig. 2. Representative images of World Health Organization grade 1 transitional meningioma at right frontal lobe, heterogenous in consistency (area 1: anterior portion; area 2: posterior portion). Conventional contrast-enhanced MR shows two distinctive areas of similar signal intensity on T1-weighted, T2-weighted, diffusion-weighted, and contrast-enhanced images, whereas MRE indicates tumor heterogeneity, firmer anteriorly (area 1: 3.2 ± 0.24 kPa) and softer posteriorly (area 2: 1.6 ± 0.34 kPa). Hematoxylin-eosin staining (original magnification, 40x) confirms greater tumor cellularity and fibrous content in area 1.

Table 2
Performance of 3D-MRE in meningioma characterization.

Parameter	AUC	Sensitivity	Specificity	PPV	NPV
Firmness	0.879 (0.792–0.938)	83.6 (71.9–91.8)	85.7(67.3–96.0)	92.7 (82.4–98.0)	70.6 (52.5–84.9)
Heterogeneity	0.773 (0.672–0.855)	54.55 (38.8–69.6)	100.0 (92.1–100.0)	100.0 (85.8–100.0)	69.2 (56.6–80.1)
Atypicality*	0.723 (0.618–0.813)	93.3 (68.1–99.8)	52.7 (40.7–64.4)	28.6 (16.6–43.3)	97.5 (86.8–99.9)
Fibroplasia**	0.835 (0.730–0.911)	100.0 (75.3–100.0)	59.0 (45.7–71.4)	34.2 (19.6–51.4)	100.0 (90.3–100.0)

*Includes atypical and anaplastic meningiomas.
**Includes fibroblastic meningiomas.
Cutpoints based on ROC curve analysis, 95% confidence intervals in parentheses.
ROC, receiver operating characteristic; AUC, area under ROC curve; PPV, positive predictive value; NPV, negative predictive value.

typical meningiomas, fibroblastic variants showed the highest stiffness levels (4.35 [IQR:3.7,6.5] kPa), followed by transitional (3.69 [IQR:2.94,4.43] kPa) and then meningothelial (2.77 [IQR:1.94,3.33] kPa) histotypes. Observed differences in meningothelial vs fibroblastic and in transitional vs meningothelial meningiomas were significant ($p < 0.001$, both), but fibroblastic and transitional variants did not differ significantly ($p = 0.06$) (Fig. 1C).

Meningothelial tumors had little or no fibrous content. However, their tumor shear stiffness ranging from very soft (1.57 kPa) to intermediate (4.5 kPa), strongly correlated with tumor cellularity ($r = 0.83$; $p < 0.001$) (Fig. 3). Transitional (or mixed) tumors were more varied in meningothelial and fibrous content, ranging from 2.35 to 8.69 kPa (Fig. 4). Although fibroblastic meningiomas (Fig. 5) varied widely in shear stiffness (3.0–12.6 kPa), they were consistently firmer than cerebrum, whether by MRE or by surgical evaluation. The rare angiomatous (n = 2) and microcystic (n = 1) tumors had the stiffness values of 2.47 kPa, 2.87 kPa, and 2.45 kPa, respectively, scored as 1–2 of tumor consistency.

MRE performed well in distinguishing fibroblastic tumors from other histotypes (AUC = 0.835, 95 % CI: 0.730–0.911; $p < 0.001$) (Fig. 1E), outperforming four conventional sequences tested ($p = 0.004$–0.04). In terms of distinguishing grades 2–3 and grade 1 meningiomas (AUC = 0.723, 95 % CI: 0.618–0.813; $p < 0.001$), it fared no better than other sequences (Fig. 1F).

4. Discussion

The current study demonstrates that MR elastography is capable of accurately measuring meningioma consistency prior to surgery. MRE may thus help detect firmness and spatial heterogeneity within tumors. MRE-derived shear stiffness also corresponded histologically with fibrous content and tumor cellularity. Although this allowed differentiation of fibroblastic meningiomas from other meningioma histotypes, atypical or anaplastic meningiomas were not separable from typical meningiomas.

Dozens of studies have utilized various MR sequences in predicting tumor consistency, citing T2WI characteristics primarily (Chen et al., 1992; Suzuki et al., 1994). At least one publication has further documented that tumor characteristics on T2WI ($p = 0.005$) and FLAIR ($p = 0.041$) (Sitthinamsuwan et al., 2012) do correlate with consistency. Still, no correlation has been shown between tumor consistency and degree of peripheral edema on contrast-enhanced imaging (Chen et al., 1992). In our study, we included a number of standardized MR techniques (T1WI, T2WI, T1WI + C, DWI), none of which proved acceptable in determining

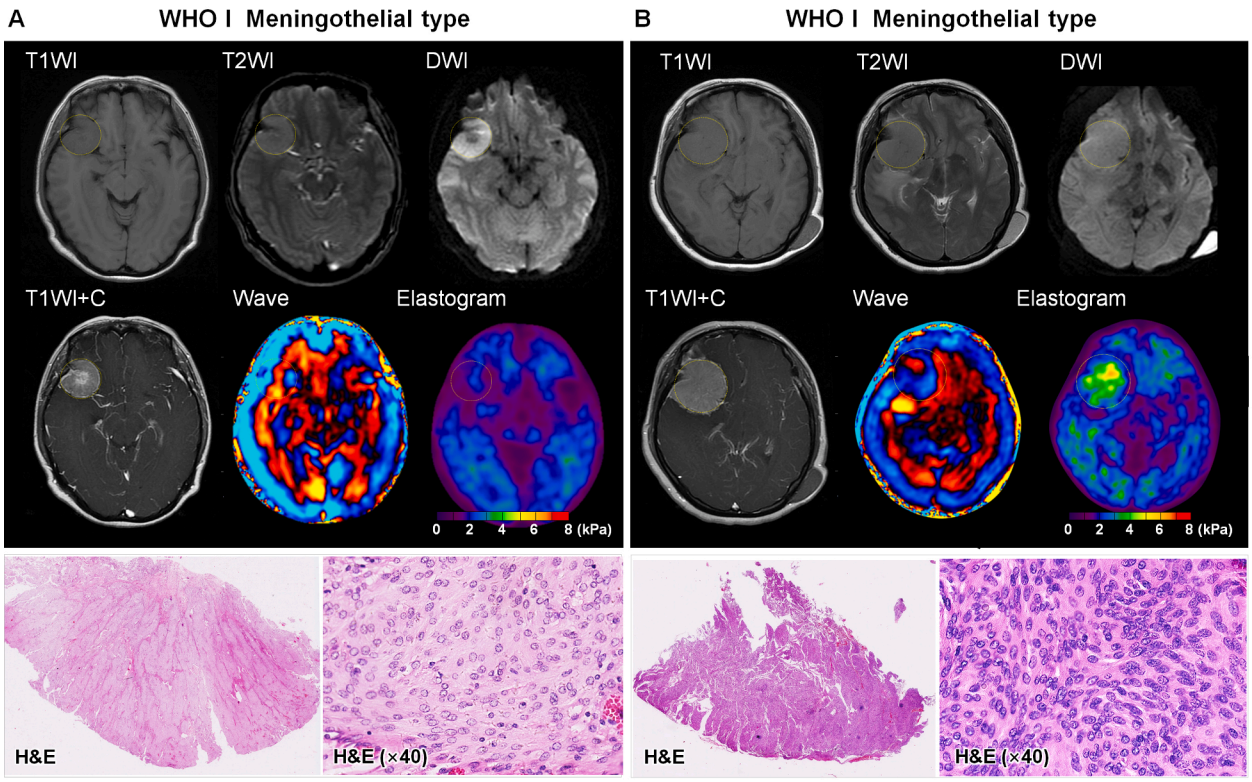

Fig. 3. (A) 48-year-old woman with World Health Organization (WHO) grade 1 meningothelial meningioma of right frontotemporal lobe. Pre-contrast T1- and T2-weighted MR (magnetic resonance) images show a mostly homogenous, isointense, round tumor with clear border. Diffusion-weighted images reveal hyperintensity. In T1-weighted MR views, there is ready enhancement, particularly at central core. Shear stiffness by MR elastography was 1.85 ± 0.32 kPa. Intraoperatively, the tumor was easily suctioned and consistent throughout. In hematoxylin & eosin (HE)-stained sections, the neoplastic cells closely resemble arachnoid cap cells, displaying round or oval, centrally placed nuclei and abundant cytoplasm. Cellularity is low level (986 cells, 40x magnification); (B) 53-year-old woman with WHO grade 1 meningothelial meningioma, again in right frontotemporal lobe. Similar signal intensity is evident on pre-contrast T1- and T2-weighted images. Diffusion-weighted imaging shows lower signal intensity than the tumor above and more homogeneous enhancement. MR elastography indicates a stiffer tumor (3.87 ± 0.72 kPa). Intraoperatively, the tumor required some degree of mechanical debulking, cauterization and full decompression. In HE-stained sections, neoplastic cells resembled those above, with approximately twice the density (2120 cells, 40x magnification).

tumor consistency (AUC range, 0.5–0.65).

It has been reported that about one-half of meningiomas are heterogenous (Takamura et al., 2021), so it is very important to show internal variations via 3D consistency mapping, rather than offering mean outputs of overall tumor consistency. In an earlier study by Murphy et al (Murphy et al., 2013a), both tumor stiffness alone and the ratio of tumor stiffness to surrounding brain tissue stiffness significantly correlated with surgical assessment of tumor stiffness in 12 meningiomas, surpassing traditional T1WI and T2WI in this regard (Hoover et al., 2011). Another more recent study by Hughes et al (Hughes et al., 2015) used higher resolution MRE, generating accurate data on overall tumor consistency and internal stiffness variations. This study also underscored the limitations of MRE in angiomatous or smaller tumors (<3.5 cm), tending to underestimate shear stiffness in such instances.

In our study, we also had two angiomatous tumors of relatively low shear stiffness, corresponding with intraoperative findings (both scored as 2, relatively soft). Because there were no firm angiomatous tumors in our cohort, the question of whether firm and highly vascularized tumors are underestimated remains open to further study. Although we did exclude very small lesions (<1.5 cm) by design, tumors < 2.5 cm still presented challenges (Fig. A2). At diameters < 2 cm, these representative meningiomas (small and firm) were entirely underestimated as soft by MRE. Tumors 2–2.5 cm across had stiff cores but were underestimated peripherally, probably due to overt boundary effect. At diameters > 2.5 cm, MRE performed acceptably in measuring stiffness, the boundary effect at tolerable levels.

Because most meningiomas arise near the skull, wave images were largely well illuminated due to strong, quick wave propagation through bone. Unlike convexity or base of skull locations, illumination was poorer for those tumors situated near the ventricular system. There were also two false-positive tumors of high shear stiffness, each gauged as soft during surgery. The reason for this is unclear, indicating the need for a quantitative and objective gold standard reference.

MRE is commonly used in the staging of fibrotic diseases, such as those affecting liver or pancreas. Indeed, the hallmark of pancreatic cancer is a highly fibrous stroma. Excessive intercellular collagen and reticulin largely accounted for the tumor firmness we have demonstrated, particularly the extreme hardness confined to fibroblastic or mixed grade 1 meningiomas. Herein, we are also first to note the impact of hypercellularity on shear stiffness, observing higher shear stiffness in intensely cellular meningothelial tumors with scarcely any fibrosis (Fig. 3). In mixed tumors, both cellularity and fibrous content created stiffer consistencies (Fig. 4), causing much variability within this tumor group. They ranged from soft tumors, resembling brain parenchyma, to very hard fibrous growths. Compared with grade 1 meningiomas, grade 2–3 tumors (Fig. 6) were characterized by high mitotic rates, greater cellularity, and small cell change. Fibrosis seems to decline with increasing grade, present in 76 %, 69.5 %, and 50 % of grade 1, 2, and 3 tumors, respectively (Backer-Grondahl et al., 2012). The implications of increasing cellularity for tumor shear stiffness among WHO tumor grades are actually mitigated by relative declines in fibrosis, rendering grade 2–3 meningiomas (most ~ 3–5 kPa) slightly stiffer than brain tissue. Seldom is there extreme firmness in the latter. This phenomenon of increasing shear stiffness due to tumor cellularity has been indirectly

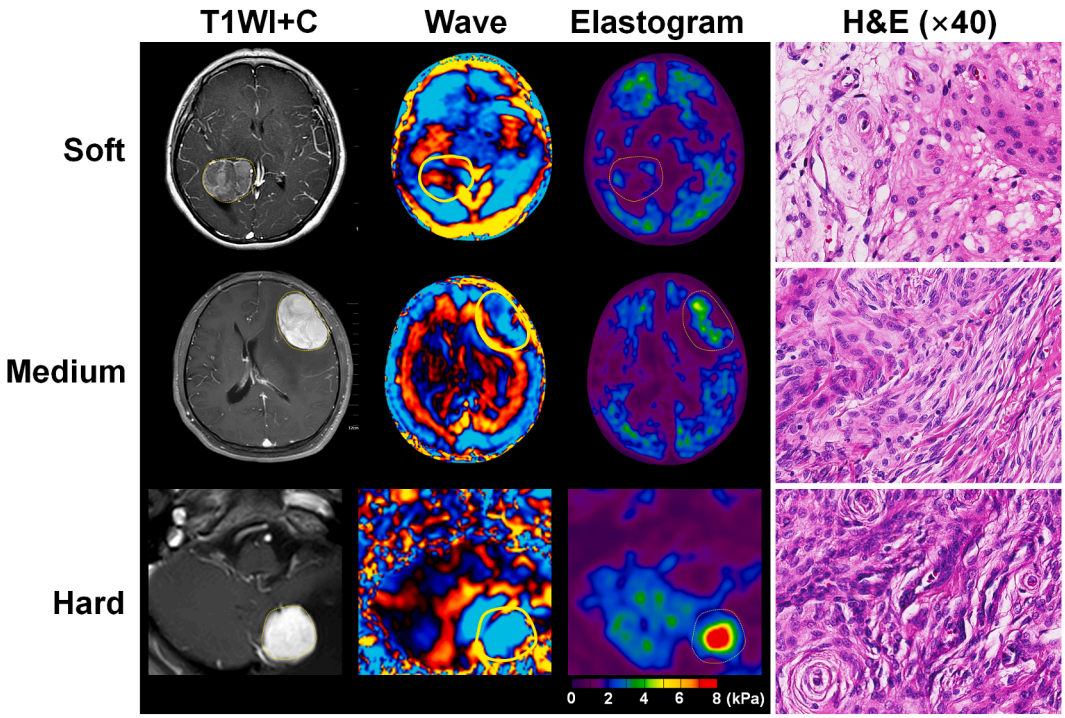

Fig. 4. Images of three World Health Organization (WHO) grade 1 transitional meningiomas that differ in consistency. Transitional meningiomas contain a mix of meningothelial and fibrous elements, here demonstrating meningothelial cells in fascicles of variable length, with fibroblastic appearance and syncytial pattern. The soft tumor (top row, 1.7 ± 0.3 kPa) of right lateral ventricle had a cell count of 713 (40x) and 20 % fibrous content; the tumor of medium consistency (middle row, 2.8 ± 0.45 kPa) in left frontal lobe appears more densely cellular, with 1543 cells (40x) and 37 % fibrous tissue; and the firm tumor (bottom row, 6.8 ± 0.74 kPa) of left cerebellum bears the densest meningothelial population, with 1843 cells (40x) and 44 % fibrous content.

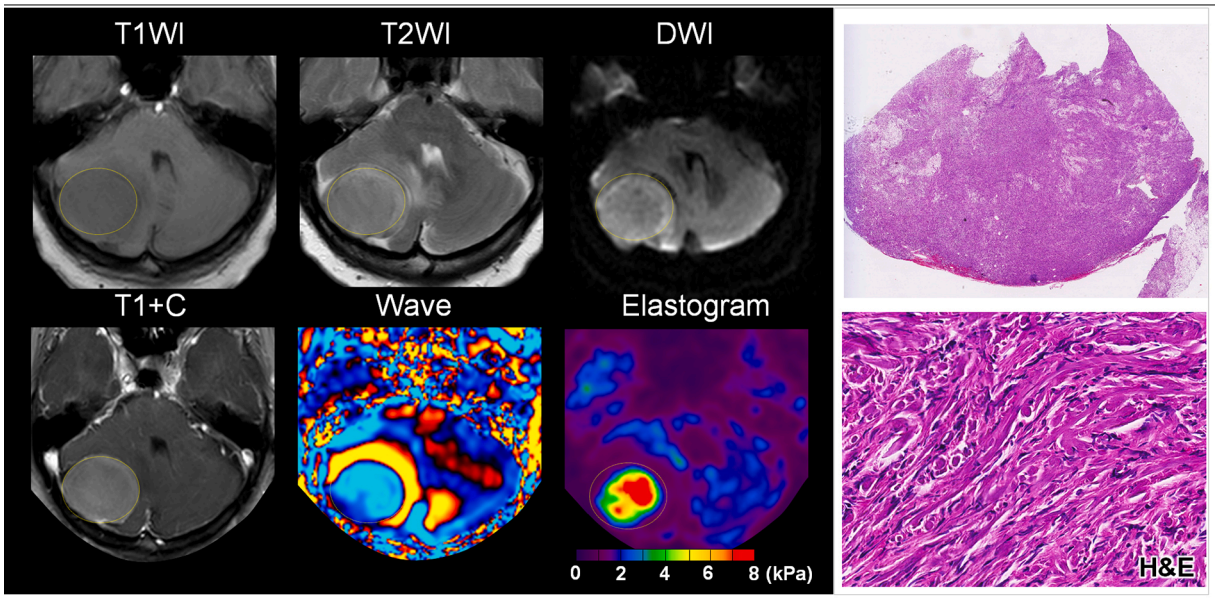

Fig. 5. Representative images from a 52-year-old man with World Health Organization (WHO) grade 1 fibroblastic meningioma of right cerebellum. Pre-contrast MR studies showed slightly low signal intensity on T1-weighted imaging, isointense signal on T2-weighted imaging, slightly hyperintense signal intensity on diffusion-weighted imaging, and moderate homogenous enhancement. By MR (magnetic resonance) elastography, the tumor was firm and homogenous (7.1 ± 0.7 kPa). Intraoperatively, tumor composition was consistent throughout, requiring cautery for complete removal. In HE-stained sections, this firm fibrous meningioma was composed of spindle cells with narrow, rod-shaped nuclei and indistinct cell boundaries, with an abundance of collagen or reticulin in the background.

illustrated in other studies (not directly as in ours). Insulinomas are regarded as very stiff tumors in the absence of fibrosis (even stiffer than pancreatic cancer), owing to extreme cellularity. Shear stiffness decreases dramatically after chemotherapy (Pepin et al., 2014; Pepin and McGee, 2018), as degrees of cellular proliferation diminish, offering an early and sensitive biomarker of tumor response to chemotherapy.

The growing prevalence of minimally invasive resection of meningiomas necessitates a non-invasive imaging technique to predict tumor consistency. In our study, meningiomas range in consistency from soft and/or suckable to very firm and/or fibrous. For convexity meningiomas

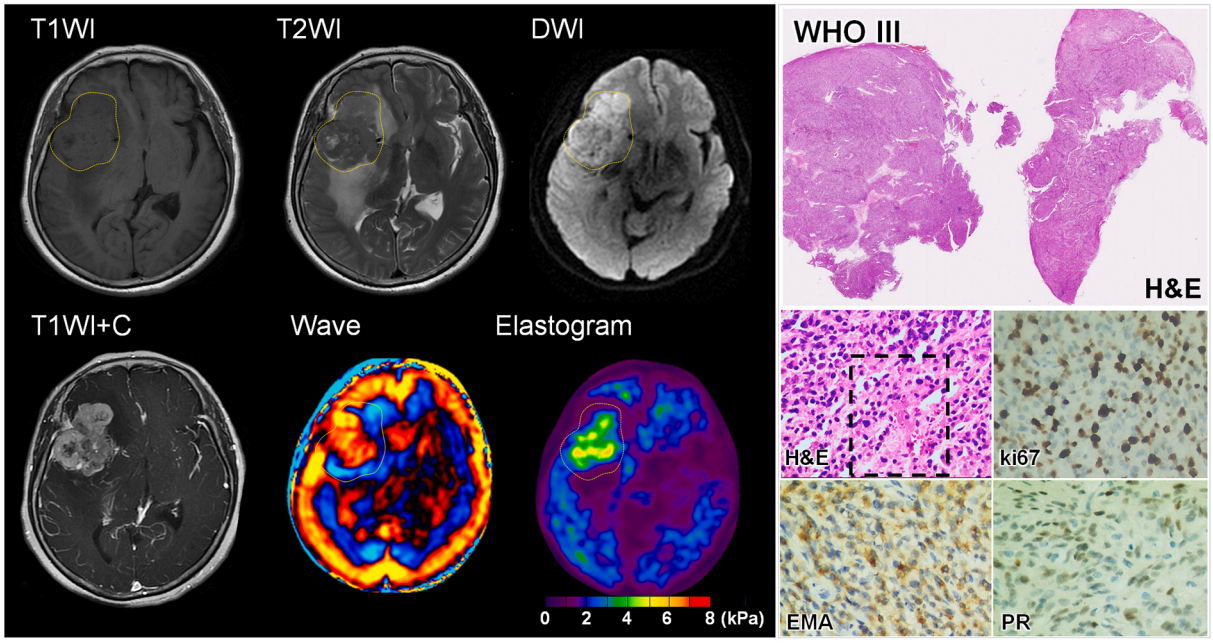

Fig. 6. Representative images from a 60-year-old man with World Health Organization (WHO) grade 3 meningioma of right frontotemporal lobe. There was heterogenous tumor signal intensity on all images (4.24 ± 1.2 kPa), mostly isointense on T1- and T2-weighted imaging and hyperintense on diffusion-weighted imaging. Ready heterogenous enhancement was observed on axial contrast-enhanced T1-weighted imaging, with signs of necrosis. Photomicrographs of the whole-slide digital image and slides digitized at 200x magnification showed a dense array of spindle-shaped cell in fascicles, along with necrosis (dashed black rectangle). Some tumor cells varied in size, showing moderate atypia. Mitotic activity in cell-dense areas was ~ 5 per 10 high-power fields (HPFs). The cytoplasm stained positive for epithelial membrane antigen (EMA), partial nuclear positivity for progesterone receptor (PR) was observed, and Ki-67 was positive over ~ 60 % of a hot spot.

/ superficial meningiomas, knowledge of consistency plays only a minor role for surgical planning or resection. However, deep-seated tumors are very difficult to access, so that tumor consistency for these tumors can be crucial for the resection strategy. From our results, the cutoff of diagnosing firm tumors or a firm portion within a tumor was 5.1 kPa. We believe that when a firm portion higher than 5.1 kPa was found, a traditional open approach may be required, especially for deep-seated tumors, such as skull-base or intraventricular meningiomas.

Certain limitations of the present study deserve mention. Although data accrued in a prospectively maintained database, histologic testing was performed retrospectively. In addition, the fact that qualitative assessments by surgeons during tumor resections served as reference standards was a clear weakness. A quantitative method would surely have been preferable. However, durometer use (as in a previous study) only generates rough estimates of Young's modulus. Another issue is that two surgeons were involved in resections, creating a potential for inconsistency; yet all were experienced meningioma surgeons, fully trained in the 5-point scoring system. MRE measurements were also only approximated with regard to intratumoral location (based on operative localization). Finally, we did not recruit a separate cohort for model validation. A broader investigation, involving an independent patient cohort from another institution, is needed to further validate our findings.

5. Conclusions

To date, this is the first study of MRE use to prospectively predict intratumoral consistency and correlate results with analogous histologic determinants. Our study provides substantial evidence, consistent with previous retrospective studies, that preoperative evaluation of meningiomas with MRE can reliably characterize tumor stiffness and spatial heterogeneity to aid neurosurgical planning. Future endeavors should aim for improved resolution of the MRE studies, resolving problems with small and deep tumors to further advance MRE as a valuable tool for preoperative planning of mengioma resection.

6. Author conflict of interest/study support

Financial support: This work was supported by the National Natural Science Foundation of China (No. 82071805); the National Youth Talent Support Program; the Innovation Talent Program in Sciences and Technologies for Young and Middle-aged Scientists of Shenyang (RC210265); the National Institutes of Health grants (R01EB001981 and R01 NS113760); and the Undergraduate Innovation and Entrepreneurship Training Program of China Medical University (Grant No S202110159013X), and the Outstanding Scientific Fund of Shengjing Hospital for study design/execution and data handling (collection, management, and analysis).

7. Data and code availability statements

All data in support of study findings are available upon request, directed to the corresponding author (pending local ethics committee approval). Because such information may compromise the privacy of research participants, public access is restricted.

Yu Shi: study concepts/study design or data acquisition or data analysis/interpretation, manuscript drafting, statistical analysis. **Yunlong Huo**: data acquisition or data analysis/interpretation, pathological analysis, manuscript revision for important intellectual content. **Chen Pan**: data acquisition or data analysis/interpretation, manuscript revision for important intellectual content. **Yafei Qi**, pathological analysis, manuscript revision for important intellectual content. **Ziying Yin**, MR elastography data analysis, manuscript revision for important intellectual content. **Richard L. Ehman**: technical support of MR elastography, manuscript revision for important intellectual content. **Zhenyu Li**: clinical studies, manuscript revision for important intellectual content. **Xiaoli Yin**, literature research, manuscript revision for important intellectual content. **Bai Du**, statistical analysis, manuscript drafting.

Ziyang Qi, clinical studies, manuscript editing. **Yang Hong**: Guarantors of integrity of entire study, clinical studies, manuscript revision for important intellectual content.

Declaration of Competing Interest

The Mayo Clinic and RLE have intellectual property rights and a financial interest related to MRE technology.

Data availability

Data will be made available on request.

Appendix A. Supplementary data

Supplementary data to this article can be found online at https://doi.org/10.1016/j.nicl.2022.103173.

References

Alyamany, M., Alshardan, M.M., Jamea, A.A., ElBakry, N., Soualmi, L., Orz, Y., 2018. Meningioma Consistency: Correlation Between Magnetic Resonance Imaging Characteristics, Operative Findings, and Histopathological Features. Asian J. Neurosurg. 13, 324–328.

Backer-Grondahl, T., Moen, B.H., Torp, S.H., 2012. The histopathological spectrum of human meningiomas. Int. J. Clin. Exp. Pathol. 5, 231–242.

Cepeda, S., Arrese, I., Garcia-Garcia, S., Velasco-Casares, M., Escudero-Caro, T., Zamora, T., Sarabia, R., 2021. Meningioma Consistency Can Be Defined by Combining the Radiomic Features of Magnetic Resonance Imaging and Ultrasound Elastography. A Pilot Study Using Machine Learning Classifiers. World Neurosurg. 146, e1147–e1159.

Chakraborty, A., Bamber, J.C., Dorward, N.L., 2012. Slip elastography: a novel method for visualising and characterizing adherence between two surfaces in contact. Ultrasonics 52 (3), 364–376.

Chen, T.C., Zee, C.S., Miller, C.A., Weiss, M.H., Tang, G., Chin, L., Levy, M.L., Apuzzo, M. L., 1992. Magnetic resonance imaging and pathological correlates of meningiomas. Neurosurgery 31, 1015–1021 discussion 1021–1012.

Clayton, E.H., Genin, G.M., Bayly, P.V., 2012. Transmission, attenuation and reflection of shear waves in the human brain. J. R. Soc. Interface 9 (76), 2899–2910.

Hoover, J.M., Morris, J.M., Meyer, F.B., 2011. Use of preoperative magnetic resonance imaging T1 and T2 sequences to determine intraoperative meningioma consistency. Surg. Neurol. Int. 2 (1), 142.

Hsu, C.-C., Pai, C.-Y., Kao, H.-W., Hsueh, C.-J., Hsu, W.-L., Lo, C.-P., 2010. Do aggressive imaging features correlate with advanced histopathological grade in meningiomas? J. Clin. Neurosci. 17 (5), 584–587.

Hughes, J.D., Fattahi, N., Van Gompel, J., Arani, A., Meyer, F., Lanzino, G., Link, M.J., Ehman, R., Huston, J., 2015. Higher-Resolution Magnetic Resonance Elastography in Meningiomas to Determine Intratumoral Consistency. Neurosurgery 77, 653-658; discussion 658-659.

Itamura, K., Chang, K.E., Lucas, J., Donoho, D.A., Giannotta, S., Zada, G., 2018. Prospective clinical validation of a meningioma consistency grading scheme: association with surgical outcomes and extent of tumor resection. J. Neurosurg. 1–5.

Kashimura, H., Inoue, T., Ogasawara, K., Arai, H., Otawara, Y., Kanbara, Y., Ogawa, A., 2007. Prediction of meningioma consistency using fractional anisotropy value measured by magnetic resonance imaging. J. Neurosurg. 107 (4), 784–787.

Manduca, A., Oliphant, T.E., Dresner, M.A., Mahowald, J.L., Kruse, S.A., Amromin, E., Felmlee, J.P., Greenleaf, J.F., Ehman, R.L., 2001. Magnetic resonance elastography: non-invasive mapping of tissue elasticity. Med. Image Anal. 5 (4), 237–254.

Murphy, M.C., Huston 3rd, J., Glaser, K.J., Manduca, A., Meyer, F.B., Lanzino, G., Morris, J.M., Felmlee, J.P., Ehman, R.L., 2013a. Preoperative assessment of meningioma stiffness using magnetic resonance elastography. J. Neurosurg. 118, 643–648.

Murphy, M.C., Huston, J., Jack, C.R., Glaser, K.J., Senjem, M.L., Chen, J., Manduca, A., Felmlee, J.P., Ehman, R.L., Barnes, G., 2013b. Measuring the characteristic topography of brain stiffness with magnetic resonance elastography. PLoS ONE 8 (12), e81668.

Muthupillai, R., Lomas, D.J., Rossman, P.J., Greenleaf, J.F., Manduca, A., Ehman, R.L., 1995. Magnetic resonance elastography by direct visualization of propagating acoustic strain waves. Science 269 (5232), 1854–1857.

Papazoglou, S., Hamhaber, U., Braun, J., Sack, I., 2008. Algebraic Helmholtz inversion in planar magnetic resonance elastography. Phys. Med. Biol. 53 (12), 3147–3158.

Pepin, K.M., Chen, J., Glaser, K.J., Mariappan, Y.K., Reuland, B., Ziesmer, S., Carter, R., Ansell, S.M., Ehman, R.L., McGee, K.P., 2014. MR elastography derived shear stiffness–a new imaging biomarker for the assessment of early tumor response to chemotherapy. Magn. Reson. Med. 71 (5), 1834–1840.

Pepin, K.M., McGee, K.P., 2018. Quantifying Tumor Stiffness With Magnetic Resonance Elastography: The Role of Mechanical Properties for Detection, Characterization, and Treatment Stratification in Oncology. Top. Magn. Reson. Imaging 27, 353–362.

Phuttharak, W., Boonrod, A., Thammaroj, J., Kitkhuandee, A., Waraasawapati, S., 2018. Preoperative MRI evaluation of meningioma consistency: A focus on detailed architectures. Clin. Neurol. Neurosurg. 169, 178–184.

Riemenschneider, M.J., Perry, A., Reifenberger, G., 2006. Histological classification and molecular genetics of meningiomas. Lancet Neurol. 5 (12), 1045–1054.

Shiroishi, M.S., Cen, S.Y., Tamrazi, B., D'Amore, F., Lerner, A., King, K.S., Kim, P.E., Law, M., Hwang, D.H., Boyko, O.B., Liu, C.-S., 2016. Predicting Meningioma Consistency on Preoperative Neuroimaging Studies. Neurosurg. Clin. N. Am. 27 (2), 145–154.

Sinkus, R., Tanter, M., Xydeas, T., Catheline, S., Bercoff, J., Fink, M., 2005. Viscoelastic shear properties of in vivo breast lesions measured by MR elastography. Magn. Reson. Imaging 23 (2), 159–165.

Sitthinamsuwan, B., Khampalikit, I., Nunta-aree, S., Srirabheebhat, P., Witthiwej, T., Nitising, A., 2012. Predictors of meningioma consistency: A study in 243 consecutive cases. Acta Neurochir. (Wien) 154 (8), 1383–1389.

Smith, K.A., Leever, J.D., Chamoun, R.B., 2015. Predicting Consistency of Meningioma by Magnetic Resonance Imaging. J. Neurol. Surg. B Skull Base 76, 225–229.

Smith, K.A., Leever, J.D., Hylton, P.D., Camarata, P.J., Chamoun, R.B., 2017. Meningioma consistency prediction utilizing tumor to cerebellar peduncle intensity on T2-weighted magnetic resonance imaging sequences: TCTI ratio. J. Neurosurg. 126 (1), 242–248.

Suzuki, Y., Sugimoto, T., Shibuya, M., Sugita, K., Patel, S.J., 1994. Meningiomas: correlation between MRI characteristics and operative findings including consistency. Acta Neurochir. (Wien) 129, 39–46.

Takamura, T., Motosugi, U., Ogiwara, M., Sasaki, Y., Glaser, K.J., Ehman, R.L., Kinouchi, H., Onishi, H., 2021. Relationship between Shear Stiffness Measured by MR Elastography and Perfusion Metrics Measured by Perfusion CT of Meningiomas. AJNR Am. J. Neuroradiol. 42, 1216–1222.

Xu, L., Lin, Y., Han, J.C., Xi, Z.N., Shen, H., Gao, P.Y., 2007. Magnetic resonance elastography of brain tumors: preliminary results. Acta Radiol. 48, 327–330.

Yamada, H., Tanikawa, M., Sakata, T., Aihara, N., Mase, M., 2021. Usefulness of T2 Relaxation Time for Quantitative Prediction of Meningioma Consistency. World Neurosurg.

Yao, A., Pain, M., Balchandani, P., Shrivastava, R.K., 2018. Can MRI predict meningioma consistency?: a correlation with tumor pathology and systematic review. Neurosurg. Rev. 41, 745–753.

Zada, G., Yashar, P., Robison, A., Winer, J., Khalessi, A., Mack, W.J., Giannotta, S.L., 2013. A proposed grading system for standardizing tumor consistency of intracranial meningiomas. Neurosurg. Focus 35, E1.